In vitro investigation of the photoprotection mechanism of Light Harvesting Complex II

Crisafi, E.

CHAPTER 2

Disentangling protein and lipid interactions that control a molecular switch in photosynthetic light harvesting

This chapter is published as E. Crisafi, A. Pandit, Biochimica et Biophysica Acta Biomembranes, 2017

Cryo-electron microscopy experiments were performed in collaboration with the Electron Microscopy Department, Groningen Biomolecular Sciences and Biotechnology, Univ. of Groningen.

ABSTRACT

In the photosynthetic apparatus of plants and algae, the major Light-Harvesting Complexes (LHCII) collect excitations and funnel these to the photosynthetic reaction centre where charge separation takes place. In high-light, remodelling of the photosynthetic membrane and protein conformational changes produce a photoprotective state in which excitations are rapidly quenched to avoid photodamage.

The quenched states are associated with protein aggregation in the membrane, however, the LHCII complexes are also proposed to have an intrinsic capacity to shift between light harvesting and fluorescence-quenched conformational states. To disentangle the effects of protein-protein and protein-lipid interactions on the LHCII photoprotective switch, we compared the structural and fluorescent properties of LHCII lipid nanodiscs and proteoliposomes with very low protein to lipid ratios. We demonstrate that LHCII proteins adopt a fully fluorescent state in nanodiscs and in proteoliposomes with highly diluted protein densities. The increase of protein density induces a transition to a mildly-quenched state that reaches a fluorescence quenching plateau at a molar protein-to-lipid ratio of 0.001 and has a fluorescence yield reminiscent of the light-harvesting state *in vivo*. The low onset for quenching strongly suggests that LHCII-LHCII attractive interactions occur inside membranes. The transition at low protein densities does not involve strong changes in the excitonic circular dichroism spectrum and is distinct from a transition occurring at very high protein densities that comprises strong fluorescence quenching and circular dichroism spectral changes involving chlorophyll *a*611 and *a*612, correlating with proposed quencher sites of the photoprotective mechanisms.

INTRODUCTION

Photosynthetic light-harvesting antennae form supra-molecular arrays with strong connectivity that capture sunlight and transfer the excitations over long distances towards the photosynthetic reaction centres, where charge separation takes place [1]. In contrast to artificial solar antennae, natural light-harvesting structures are dynamic assemblies that continuously adapt to the light conditions for prevention of photodamage [2]. In the excess of light, extensive remodelling of the photosynthetic thylakoid membranes takes place. The ability of the peripheral Light-Harvesting Complexes of plants and photosynthetic algae to adapt fluorescent, light harvesting, versus photoprotective, excitation-quenched states under excess light conditions, is a phenomenon that has been studied extensively *in vivo* and *in vitro* over the last decades [3-9]. LHCII proteins have the intrinsic capacity to switch between light-harvesting, fluorescent, or photoprotective, quenched conformational states [4,10]. The formation of quenched states is associated with LHCII aggregation in the membrane and the balance between light harvesting and photoprotection is regulated by membrane remodelling in high light conditions [8,11]. Mild dilution with thylakoid lipids of overcrowded mutant thylakoid membranes has shown to increase the LHCII chlorophylls (Chls) fluorescence lifetimes, while further dilution functionally uncouples the LHCII antenna proteins from the photosystem reaction-center units [12,13]. Thus, the functional roles of the light-harvesting proteins to transfer excitations to the photosynthetic reaction centres or dissipate excess excitations under high light critically depend on the respective protein to lipid densities within strong- or weak-coupling regimes. The strong correlation between quenching and protein aggregation *in vivo* and *in vitro* together with the notice that individual LHCII complexes can adopt different fluorescent states, suggests a mechanistic process in which external pressure and protein or lipid changes in the LHCII microenvironment bring about a molecular conformational change. This change should involve altered Chl-Cars or Chl-Chl interactions to be able to quench the light excitations [5,14,15]. While several models have been proposed for the photophysical quenching mechanisms [5,14-16] involving the protein-bound Chls, lutein and/or zeaxanthin, there is no clear view on the mechanistic process or on the protein conformational switch that is associated with a twist in the protein-bound neoxanthin (Neo), a change in Chl *b* hydrogen bond strength [14], subtle changes in the Chl *a* ground-state electronic structures [17,18] or conformational changes in one of the luteins (Lut1) [19]. Upcoming methods, like single-molecule fluorescence and nuclear magnetic resonance (NMR), are being explored to comprehend the conformational switch of LHCII and its associated mechanistic process [4,17]. The relevance of such studies strongly relies on the chosen *in vitro* conditions to mimic the *in vivo* membrane environment. In addition, new kinetic models have been proposed that describe excitation, diffusion, and quenching in small LHCII aggregates, that benefit from experimental data describing the behaviour of single and aggregated LHCII under controlled, membrane-mimicking conditions [20,21].

Model lipid membranes form suitable tools for the investigation of protein structure, dynamics and lipid interplay in a controlled environment and open the possibility to

create artificial minimal protein networks with functional connectivity. LHCII-reconstituted proteoliposomes and protein-lipid aggregates have been investigated to determine inter-protein connectivity and protein-lipid interactions under various conditions [22-24]. Comparing the structural and functional properties of aggregated membrane proteins in proteoliposomes with those of isolated proteins embedded in detergent micelles, however, creates a bias because the protein microenvironment changes when proteins are transferred from detergent micelles to lipid membranes. Lipid nanodiscs form attractive alternative model systems that prevent protein aggregation while providing a lipid environment. We demonstrated that LHCII proteins could be reconstituted in asolectin lipid nanodiscs, capturing the proteins in their fluorescent, light-harvesting state [25].

In this chapter, we compared both structure and fluorescence properties between LHCII in lipid nanodiscs and LHCII in proteoliposomes, thereby disentangling protein-protein and protein-lipid interactions in minimal membrane models to investigate the LHCII mechanistic, functional switch. The LHCII pigment-protein complexes are unique in possessing Chls and xanthophylls that form intrinsic probes, reporting changes in the microenvironment. By adjusting the protein to lipid ratio (PLR) in the proteoliposomes, we determined the onset ratio for protein aggregation in membranes, bridging the gap between properties of isolated proteins and of their aggregated states. Liposome and nanodisc models were prepared from plant thylakoid or from soybean asolectin lipids to investigate the influence of specific lipid microenvironments. Thylakoid lipids were used to mimic the lipid composition of native thylakoid membranes. Preparations of soybean asolectin lipids were used as easily controllable lipid model systems and for comparison of our data with previous results obtained in an earlier study on LHCII lipid nanodiscs [25]. Circular dichroism (CD) experiments were carried out to characterize LHCII pigment interactions for the different membrane model systems.

MATERIALS AND METHODS

LHCII EXTRACTION

Light-Harvesting Complexes were purified from *Spinacia oleracea* leaves as previously described [25]. In short, LHCII trimer complexes were isolated using a sucrose gradient. The green band of LHCII trimers was manually collected with a long needle. The purified LHCII complexes were characterized by absorption spectroscopy. The sucrose buffer was exchanged into buffer containing HEPES 50 mM, NaCl 100 mM, pH 7.5, *n*-Dodecyl *β*-D-maltoside (*β*-DM, Sigma) 0.03%. The solution was concentrated using Amicon Ultra 2 mL centrifugal filters with a cut off of 30 kDa (Millipore). The protein complexes were stored at -80°C until use.

PREPARATION OF ASOLECTIN LIPOSOMES

Chloroform was added to asolectin from soybean lipids (Sigma) to a concentration of 5 mg/ml. The chloroform/asolectin solution was collected in a round-bottom flask, and all solvent was evaporated with a stream of N_2 followed by evaporation in a rotary evaporator (R3000, Buchi). The phospholipid bilayer was then hydrated using the reverse phase method [26]. A solution was poured to the dried film containing the buffer (HEPES 50 mM, NaCl 100 mM, pH 7.5) and diethyl ether in the ratio 1 to 3, and gently mixed and sonicated (2210, Branson). The diethyl ether was evaporated using the rotary evaporator and the last traces of solvent were removed using a stream of N_2. The liposome suspensions were exposed to 10 freeze/thaw cycles followed by extrusion through polycarbonate membranes of 400 and 200 nm pore size, using a mini-extruder (Avanti polar lipids). Sizes of liposome preparations were determined by dynamic light scattering (DLS, Malvern Zetasizer Nano ZS) equipped with a thermostatic cell holder controlled by a Peltier element.

PREPARATION OF THYLAKOID-LIPID LIPOSOMES

Thylakoid lipids phosphatidylglycerol (PG), digalactosyldiacylglycerol (DGDG), monogalactosyldiacylglycerol (MGDG) and sulphoquinovosyl diacylglycerol (SQDG) were purchased from Lipid Products Company (Redhill). Unilamellar liposomes were prepared according to [27]. Lipid mixtures containing 47% MGDG, 27% DGDG, 12% SQDG and 14% PG were dried into a thin film using a rotary evaporator at 40°C, to remove all traces of chloroform. The lipid film was hydrated using a reconstitution buffer (HEPES 50 mM, NaCl 100 mM, pH 7.5 and 0.03% β-DM) to a final lipid concentration of 0.25 mg/ml. Detergent was extracted by incubation for 48 hrs with polystyrene beads (Bio-beads, SM-2, Bio-Rad). The liposome suspensions were exposed to 10 freeze-thaw cycles followed by extrusion through polycarbonate membranes with 200 nm and 100 nm pore sizes.

PROTEIN INSERTION IN LIPOSOMES

To determine the onset of liposome solubilisation by detergent, liposome preparations were titrated with β-DM and DLS and 90° light scattering were used to monitor the solubilisation of liposomes into lipid-detergent micelles.

Liposome solubilisation curves were obtained by mixing liposomes with increased amounts of β-DM. Solubilisation of the liposome vesicles into lipid-detergent micelles upon detergent titration was followed by the decrease of 90° light scattering measured with a fluorescence spectrometer (Varian) with the excitation and detection wavelength both set at 500 nm (Figure 2.1). Particle sizes of the liposome-detergent preparations were determined by DLS. The onset value for solubilisation was determined as 0.01% β-DM for liposome preparations containing 0.95 mM lipid, which converts to 5 lipids per detergent molecule.

For protein insertion, preformed liposomes were destabilized by the addition of 0.03% of β-DM to facilitate the insertion of LHCII into the membranes. LHCII complexes were added to the suspension and incubated for 30 min. For proteoliposomes preparations with

high PLRs (1:65), instead of insertion into preformed liposomes, the LHCII complexes in β-DM were directly mixed with detergent-solubilized lipids. Bio-beads were added to the suspensions in several steps and solutions were incubated overnight. The proteoliposomes suspension was centrifuged at 15000 x g for 30 minutes at 4°C using a table-centrifuge (5430 R, Eppendorf) to remove non-incorporated LHCII that forms aggregate pellets.

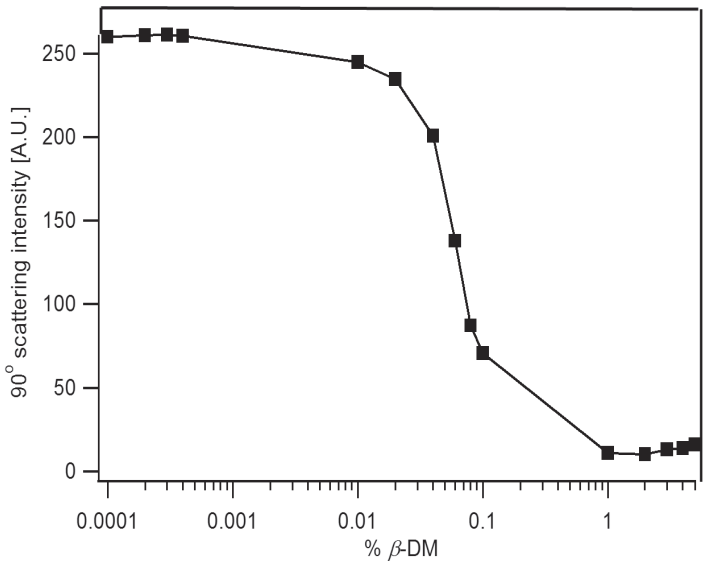

Figure 2.1 Solubilisation of asolectin liposomes (lipid 0.95 mM) upon β-DM titration. The onset of solubilisation starts at β-DM 0.01%.

Preparations of LHCII in 0.03% β-DM and of LHCII proteoliposomes were loaded on sucrose gradients 10-45% and run overnight at 200000 x g at 4 °C in an SW41 rotor (Beckmann). Figure 2.2 shows that LHCII proteoliposomes form two bands on the sucrose gradient, while there are no visible LHCII aggregates at the bottom of the tube, confirming that all of the LHCIIs were incorporated.

The proteoliposome preparations were characterized by cryo-electron microscopy (cryo-EM, FEI Technai T20 electron microscope, operating at 200 keV). The reported PLR is defined as moles of LHCII trimers per moles of total lipids. The concentration of LHCII was determined from the molar extinction coefficient for trimers
at 670 nm, ε=1638000 M^{-1} cm^{-1} [28].

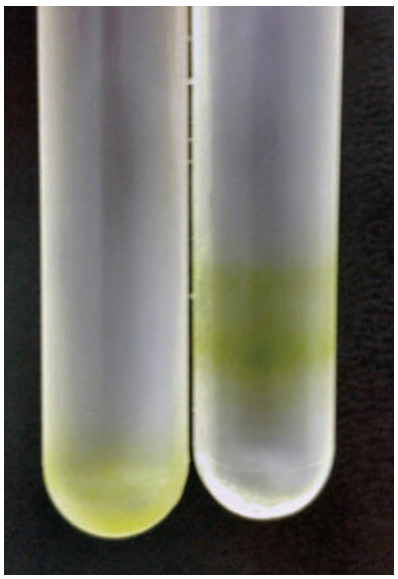

Figure 2.2 Sucrose gradient of LHCII aggregates (bottom left) and LHCII proteoliposomes with PLR = 1:65 (right).

PREPARATION OF LHCII ASOLECTIN NANODISCS

For incorporation of LHCII in lipid nanodiscs, we used the membrane scaffold protein 1E3D1 (MSP 1E3D1) [29]. MSPs are amphipathic helices and are genetically engineered apolipoproteins (A-1). The MSP1E3D1 overexpressed in *E. coli* was purification and consequentely stored at -80ºC. Lipid nanodiscs are formed spontaneously upon detergent extraction of lipid: detergent: MSP mixtures. In lipid nanodiscs, the lipid molecules associate as a bilayer domain while two molecules of MSP wrap around the edges of the discoidal structure in a belt-like configuration, one MSP covering the hydrophobic alkyl chains of each leaflet (see Figure 1.11, Chapter 1). For the preparation of LHCII asolectin nanodiscs, a 5 mg/ml solution of asolectin was prepared according to Pandit *et al.*, in buffer (HEPES 50 mM, NaCl 100 mM, pH 7.5) with nonyl β-D-glucopyranoside 40 mM (Sigma) [25]. LHCII complexes were mixed with the lipid/ detergent solution and incubated at 4°C while shaking for 15 min. The MSP1E3D1 was added to the mixture and incubated for another 15 min [25]. To allow the reconstitution of protein in nanodiscs, the detergent was removed using Bio-beads (SM-2). Samples were diluted to a final volume of 2 ml and ultra-centrifuged at 120000 x g at 4°C to remove lipid and protein pellets, in an Ultracentrifuge (Optima L-90K, Beckman) using a 70.1 Ti rotor. Because we observed that for some preparations small aggregates remained in the lower part of the supernatant, the upper and lower volumes of the 2 ml supernatant solution were collected separately from the centrifuge tubes. Sizes of empty nanodisc and liposome preparations were determined by DLS. The illumination wavelength of the DLS apparatus, 632.8 nm, was not suitable for measuring scattering profiles of LHCII-containing samples because LHCII fluorescence upon illumination at 632.8 nm interfered with the scattering profile.

PREPARATION OF LHCII THYLAKOID-LIPID NANODISCS

Nanodiscs consisting of plant thylakoid lipids were prepared as described above for asolectin lipid nanodiscs, except for the initial step. Native thylakoid membranes contain the non-bilayer lipid MGDG that makes up ~40-50% of the lipid constituents [30]. The addition of MGDG to our lipid preparations prevented the formation of nanodiscs and resulted in the formation of LHCII lipid aggregates. MGDG is a non-bilayer lipid that changes the membrane lateral pressure profile and has a preference for hexagonal membrane phases [31]. The cone-shaped MGDG lipids might prevent the formation of flat lipid membrane discs that are stabilized by the MSP proteins. Lipid mixtures containing 47% MGDG, 27% DGDG, 12% SQDG and 14% PG or lacking MGDG, containing 61.9% DGDG, 16.7% SQDG and 21.4% PG were dried with a rotary evaporator for 45 minutes at 40°C. The lipid film was hydrated with buffer (HEPES 50 mM, NaCl 100 mM, pH 7.5) containing 40 mM nonyl β-D-glucopyranoside. The remaining steps were performed following the protocol described above for asolectin lipids.

CIRCULAR DICHROISM MEASUREMENTS

CD spectra of the LHCII nanodiscs and proteoliposome suspensions were recorded with a J-815 spectropolarimeter (Jasco) equipped with a Peltier element temperature control. The wavelength range was from 350 to 750 nm, data pitch 1 nm, response 2 s, bandwidth 4 nm, and scanning speed 50 nm/min at 20°C using a 0.2 or 0.5 cm quartz cuvette (Hellma).

ABSORPTION MEASUREMENTS

Absorption spectra were recorded with a UV-1700 PharmaSpec UV-Vis spectrophotometer (Shimadzu) over a wavelength range from 350 to 750 nm

FLUORESCENCE MEASUREMENTS

Fluorescence measurements were performed with a Cary Eclipse fluorescence spectrophotometer (Varian), collecting emission spectra from 660 to 720 nm using 3 mm quartz cuvettes. The optical density of the sample preparations varied from 0.03 to 0.07 cm^{-1} at 650 nm. The excitation wavelength (λ_{ext}) was set at 650 nm or at 475 nm. Fluorescence quantum yields of LHCII proteoliposome and nanodisc preparations were determined relative to the fluorescence yield of LHCII in β-DM. Data were corrected for the number of absorbed photons by dividing the fluorescence intensities by 1-Trasmission (1-T).

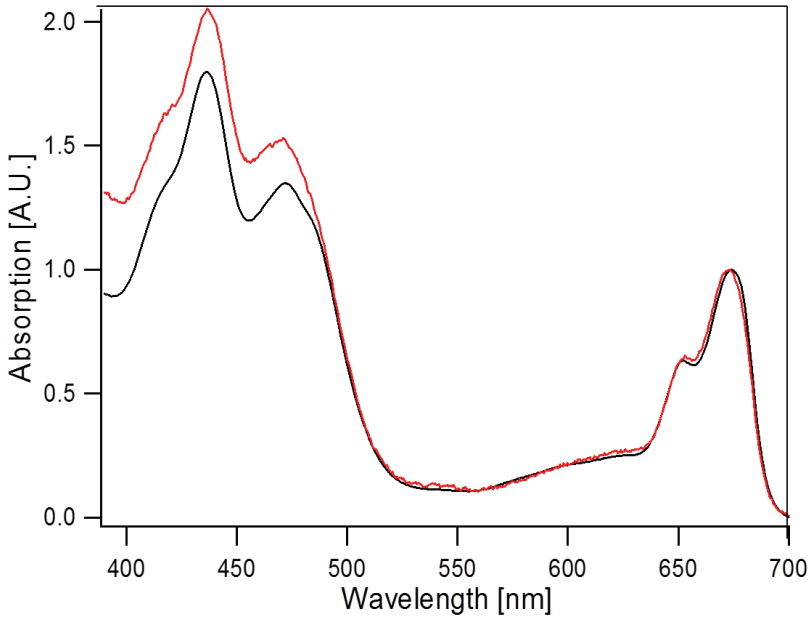

Figure 2.3 UV-VIS Absorption spectra of LHCII proteoliposomes with protein to lipid ratios of $5 \cdot 10^{-5}$ (red) and of LHCII in 0.03% β-DM (black). Spectra are normalized at the Chl a Q_y maximum.

To minimize errors caused by liposome scattering, which causes a scattering background signal at the blue side of the absorption spectra, as shown in Figure 2.1, liposome samples were excited at the red side in the Q_y band of Chl *b* (ε_{exc}= 650 nm) and fluorescence emission spectra were corrected for the number of absorbed photons dividing the fluorescence intensities by $1\text{-}T_{650}$.

RESULTS AND DISCUSSIONS

FLUORESCENCE ANALYSIS OF LHCII IN NANODISCS COMPOSED OF ASOLECTIN OR THYLAKOID- LIPIDS

Sample	LHCII: MSP: lipid	Φ/Φr (%)
1	1:4:427	100
2	1:4:213	100
3	1:12:870	70
4	1:24:870	75
5	1:12:120	90
6	1:18:180	90
7	1:20:120	74
8	1:5:120	80

Table 2.1 Fluorescence yields relative to LHCII in β-DM of LHCII nanodiscs preparations, composed of DGDG: SQDG: PG lipid mixtures (sample 1 to 4) or of soybean asolectin lipids (sample 5-8).

At optimized LHCII: MSP: lipid ratios, LHCII lipid nanodiscs prepared using asolectin or DGDG: SQDG: PG lipids had fluorescence intensities that were comparable to the fluorescence intensities of LHCII in β-DM micelles as reported in Table 2.1, while with sub-optimal LHCII: MSP: lipid ratios, lower fluorescence yields were observed, caused by the presence of small amounts of LHCII aggregates that quench the fluorescence.
Note that in lipid membranes where the LHCII proteins would not be prevented from protein-protein interactions by the MSPs, protein to lipid ratios of 1:120 or 1:180 as were used for the asolectin nanodiscs would induce quenched states of LHCII by protein aggregation [32]. In contrast, the fluorescence yields in Table 2.1 confirm that the nanodisc scaffolds prevent LHCII aggregation. In earlier work, it was already demonstrated that LHCII retains its fluorescent state upon reconstitution in asolectin nanodiscs [25]. Here we conclude that LHCII also adapts an unquenched, fully fluorescent state in nanodiscs composed of thylakoid lipids.

FLUORESCENCE ANALYSIS OF LHCII PROTEOLIPOSOMES AT LOW PROTEIN TO LIPID RATIOS

In artificial and in native membranes, the fluorescence of LHCII is reduced compared to the fluorescence of LHCII in detergent micelles. The LHCII-nanodisc experiments, however, show that the transition from a detergent to a lipid environment in itself does not produce quenched states. We reasoned that quenching of LHCII in membranes is caused by their aggregation and that very diluted concentrations of LHCII complexes in proteoliposome membranes should reproduce the fluorescence yields of the LHCII lipid nanodiscs. To test this assumption, we prepared LHCII asolectin proteoliposomes with PLRs in the range 2 x 10^{-5} to 2 x 10^{-3}. At the lowest ratios, the fluorescence yield indeed equals the fluorescence yields of LHCII in lipid nanodiscs or detergent micelles as shown in Figure 2.4. The fluorescence yield decreases with increased PLR until a plateau is reached where the yield is reduced to ~50% relative to the fluorescence of LHCII in lipid nanodiscs. This reduced yield is comparable with the reduction in fluorescence that is observed for LHCII in dark-adapted leaves *in vivo* [8,25,33].
For clarity, the x-axis in Figure 2.4 has a logarithmic scale. Data were fit with a standard sigmoidal curve to determine the midpoint PLR value, using the fit function:

$$y = Fmax - F/\{1 + \exp[(\text{xhalf-x})/\text{xo}]\}$$

The fit would give a midpoint PLR value x-half = 0.0001 (Figure 2.4). Exponential fitting was also performed and would give a half-life PLR of 0.00015 and offset y_0= 0.49 (fluorescence at plateau level). The fits at this point do not represent a functional model for concentration quenching but were used to estimate the PLR values at which mild quenching occurs and the fluorescence yield at the plateau level.

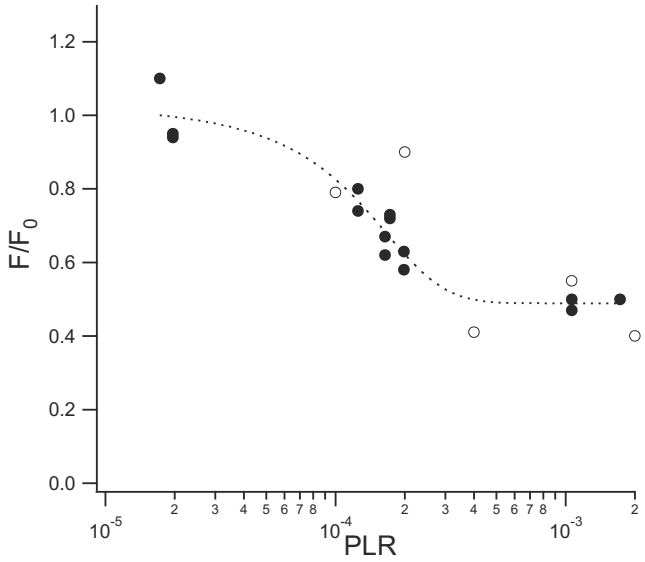

Figure 2.4 Fluorescence yield (F/F_0) of LHCII asolectin proteoliposomes (black circles) and thylakoid MGDG: DGDG: SQDG: PG proteoliposomes (open circles) relative to the fluorescence of LHCII in β-DM micelles (F_0) at a different PLR. To determine the midpoint PLR value, data were fit with a standard sigmoidal curve using the following fit parameters: half at PLR = $1.0 \cdot 10^{-4} \pm 8.2 \cdot 10^{-5}$, maximal fluorescence reduction = -0.67 ± 0.31 and Fmax = 1.16± 0.30.

The asolectin LHCII proteoliposomes in our preparations had varying sizes according to different EM micrographs in Figure 2.5.

Assuming that (1) liposomes contain double-leaflet membranes in which each asolectin lipid molecule occupies a surface area of 70 Å [34], (2) the mean diameter of the liposomes as determined by EM ranges from 60 nm to 80 nm, and (3) discarding any losses of LHCII or lipids during our preparations, we estimate that preparations with a PLR of 1×10^{-4}, which corresponds to the midpoint value of the quenching curve in Figure 2.4, contain 1 to 2 LHCII trimers *per vesicle*.

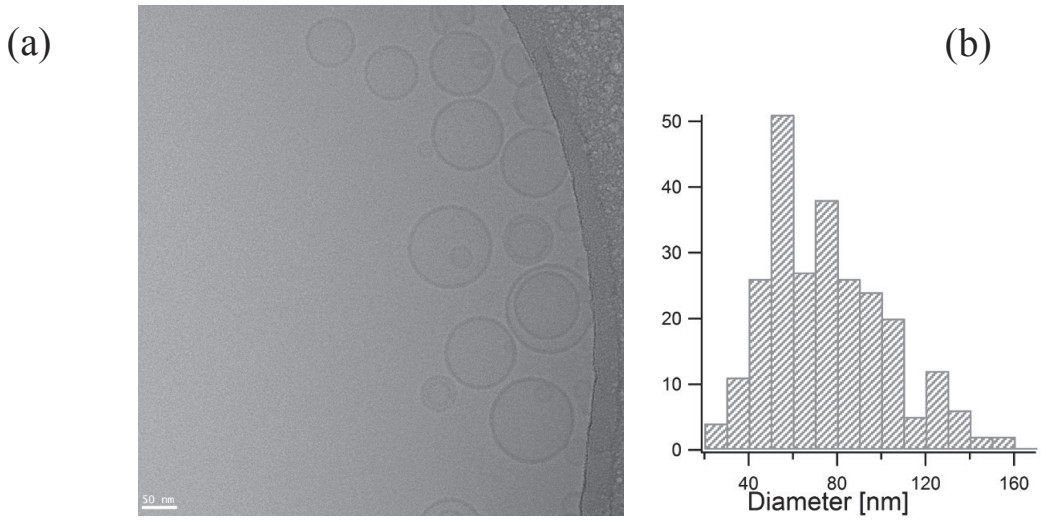

Figure 2.5 (a): Cryo-electron micrograph of asolectin LHCII proteoliposomes (scale bar 50 nm). (b): size distribution of asolectin liposomes, extracted from several electron micrographs.

The curve reaches a plateau value of ~50% quenching with on average 8-14 LHCII *per vesicle*, assuming vesicle sizes of 60-80 nm (Figure 2.5). Interestingly, the estimated average number of LHCIIs per vesicle at which the fluorescence quenching reaches a plateau (8–14 trimers) approaches the experimentally determined range for functional domain sizes of LHCII *in vivo* of 12–24 trimers, according to Lambrev *et al.* [35]. Although the calculations are a rough estimate, the numbers imply that the onset for fluorescence quenching starts when only a few LHCII complexes *per vesicle* are present, suggesting that the LHCII proteins have attractive interactions and form small aggregate clusters. Our previous study on LHCII-lipid nanodiscs showed that LHCII-lipid preparations containing disc particles with diameter sizes ranging from 12 to 50 nm, already display considerable quenching characteristics, the fluorescence yields were reduced to 40% compared to LHCII in detergent micelles [25]. Hence, small clusters of LHCII are capable of significantly reducing the fluorescence.

LHCII proteoliposomes prepared from thylakoid MGDG: DGDG: SQDG: PG lipid mixtures displayed similar quenching characteristics. For these lipid mixtures, however, it was more difficult to control the PLR without loss of protein and lipids, which was sometimes observed as small LHCII pellets after the centrifugation step, and only a few PLR values are compared (open circles in Figure 2.4). For consistency with the lipid compositions of the thylakoid lipid nanodiscs, we also prepared liposomes without MGDG. These preparations, however, contain mixtures of lipid vesicles and planar lipid sheets, as shown in Figure 2.6, and the sample was strongly quenched with a fluorescence intensity of ~20% compared to LHCII in β-DM. Summarizing, the LHCII proteoliposome data confirm that LHCII fluorescence quenching is induced by LHCII-LHCII interactions and not by a (specific) lipid microenvironment.

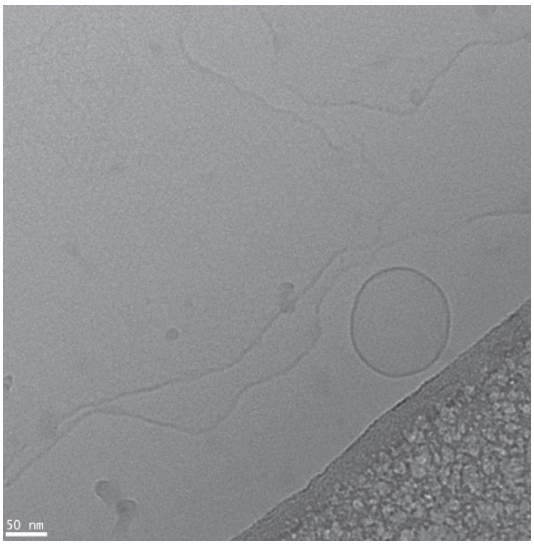

Figure 2.6 Cryo-electron micrograph of DGDG: SQDG: PG, LCHII proteoliposomes with PLR of 1.6x10^{-3}. The picture shows the co-existence of proteoliposomes and lamellar sheets.

The non-bilayer lipid MGDG has been suggested to play a role in controlling the photoprotective states of LHCII. Here we show that LHCII reconstituted in thylakoid

lipid membranes with MGDG proteoliposomes, or without MGDG nanodiscs, both adapt unquenched states. Molecular interactions between LHCII and MGDG lipids apparently do not induce fluorescence quenching. The MGDG lipids however clearly have an effect on the mesoscale organization, disturbing the thermodynamic equilibrium that stabilizes the MSP-lipid nanodisc scaffolds and counteracting the formation of large two-dimensional flat lipid-bilayer sheets. In native, highly crowded thylakoid membranes, LHCII aggregation is associated with reversible supramolecular membrane phase transitions [11]. In liposomes, MGDG and DGDG promote LHCII aggregation [22] and in LHCII-Photosystem II (PSII) liposomes, MGDG lipids increase the light-harvesting cross-section, promoting LHCII-PSII interactions [23]. These studies strongly suggest a functional role for MGDG in controlling the supramolecular interplay between light-harvesting proteins *in vivo*.

CD CHARACTERIZATION OF LHCII-NANODISCS AND LHCII-PROTEOLIPOSOMES

In LHCII pigment-protein complexes, excitonic Chl-Chl and carotenoid-Chl interactions give rise to pronounced exciton bands in the CD spectrum in the visible region [36]. The CD spectral shapes are very sensitive to the LHCII pigment-protein folds and their microenvironment [37,38]. To gain insight in the pigment-protein folds in different microenvironments and the influence of protein-lipid versus protein-protein interactions, we compared the excitonic CD spectra of LHCII in β-DM detergent micelles, lipid nanodiscs, and proteoliposomes. Figure 2.7 presents the CD spectra of LHCII in β-DM, LHCII in DGDG: SQDG: PG and asolectin nanodiscs and LHCII in MGDG: DGDG: SQDG: PG proteoliposomes with PLR of 1:555. In the Soret region, the peaks at (-)469 nm and (-)489 nm have similar intensities in the spectrum of thylakoid lipid nanodiscs, while in the spectrum of proteoliposomes, the (-)469 nm band clearly has gained more strength relative to the 489 nm band. Increase in strength of the (-)469 nm band combined with a decrease of the (-)489 nm band has been attributed to stronger inter-monomer interactions within the LHCII trimers [39,40]. The change in the 469/489 ratio observed for proteoliposomes suggests that LHCII-LHCII interactions in the membrane stabilize the trimers. The CD spectrum of asolectin nanodiscs also has a stronger (-)469 nm band than the spectrum of thylakoid lipid nanodiscs, indicating that the environment of the asolectin lipids increases the stability of the LHCII trimers.

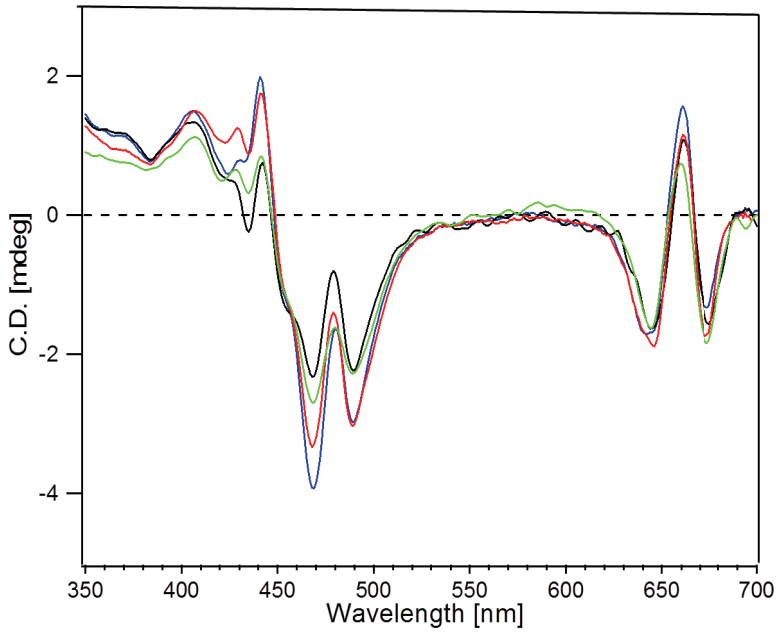

Figure 2.7 CD spectra of LHCII in β-DM (red), LHCII in MGDG: DGDG: SQDG: PG proteoliposomes (PLR 1:555, blue), LHCII in DGDG: SQDG: PG nanodiscs (black) and LHCII in asolectin nanodiscs (green).

Figure 2.8 shows CD difference spectra of LHCII thylakoid lipid nanodiscs minus LHCII in *β*-DM, and nanodiscs minus proteoliposomes. Remarkably, both difference spectra contain pronounced bands at (+)470 nm and (-)438 nm. The similar dispersive difference signal of the two difference spectra suggests that the nanodisc *itself* influences the LHCII pigment microenvironments. Considering the size of the LHCII trimer complexes, a triangular-shaped protein complex of ~6 nm wide, relative to the nanodisc dimensions of ~12 nm in diameter, the surrounding MSP proteins could be in contact with the exterior xanthophyll and Chl pigments of LHCII. These pigments are the neoxanthin (Neo) that protrudes from the protein complexes, and the Chls *b*601, *b*605, *b*606, *b*608 and *a*610, *a*611, *a*612 and *a*614 (nomenclature according to Liu *et al.* [41]). Previous work demonstrated that changes occur in the Soret and Q_y band of absorption spectra of LHCII in lipid nanodiscs compared to detergent-solubilized LHCII, uncorrelated to fluorescence quenching [25]. These changes may also be explained by LHCII pigment interactions with the surrounding MSPs.

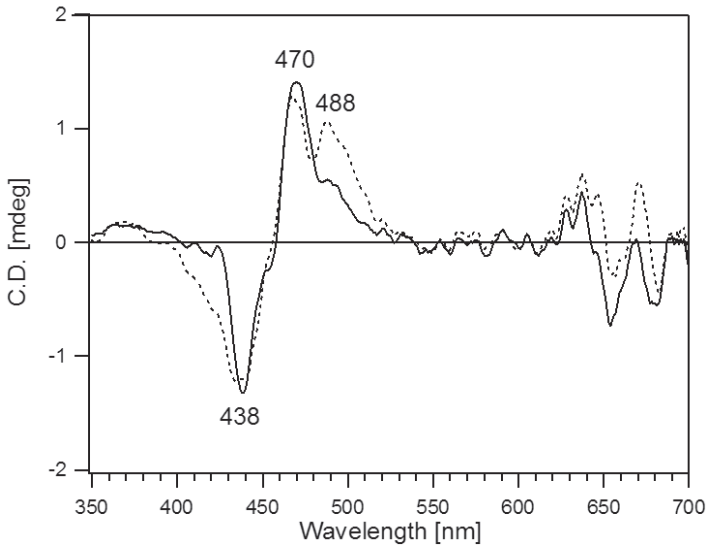

Figure 2.8 CD difference spectrum of LHCII nanodiscs minus LHCII in β-DM (dashed) and LHCII nanodiscs minus LHCII MGDG: DGDG: SQDG: PG proteoliposomes (solid line). Proteoliposomes were prepared with three different PLRs: 1:2222, 1:555 and 1:65. The two lowest PLRs are in the regime described in Figure 2.1, where the fluorescence quenching is maximal ~50%, reminiscent of the light-harvesting states in vivo in the weak-coupling regime. Instead, the fluorescence intensity of the densely packed proteoliposome preparations with PLR 1:65 is reduced to 10-15% compared to LHCII in β-DM micelles (Figure 2.9), which is comparable to photoprotective states in vivo [33].

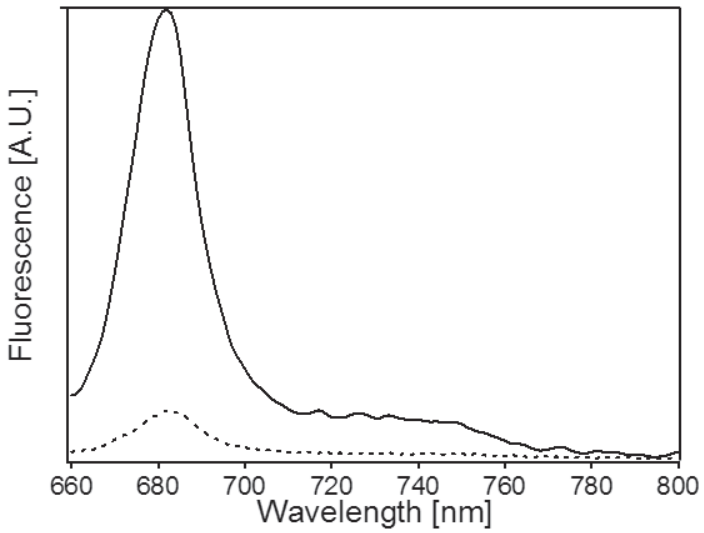

Figure 2.9 Fluorescence emission of LHCII proteoliposomes with PLR of 1:65 (dotted line) compared to LHCII in β-DM (solid line) upon 650 nm excitation. Fluorescence intensities were scaled according to their relative transmission (T) at 650 nm, by dividing by the fluorescence intensities by (1-T).

Figure 2.10 compares the CD spectra of LHCII proteoliposomes with different PLRs. The samples with PLRs of 1:2222 and 1:555 have similar excitonic CD spectra. As demonstrated in Figure 2.4, changing the PLR in this regime also has only a moderate effect on the fluorescence yields. For the sample with PLR 1:65, however, spectral changes are observed that are indicated with the black arrows. The CD spectrum of proteoliposomes with PLR 1:65 resembles reported CD spectra of LHCII proteoliposomes in other work [40]. A comparison of proteoliposomes with low and high PLRs allows us to

detect the CD changes that are associated with the transition from a mild to a strong fluorescence-quenched state.

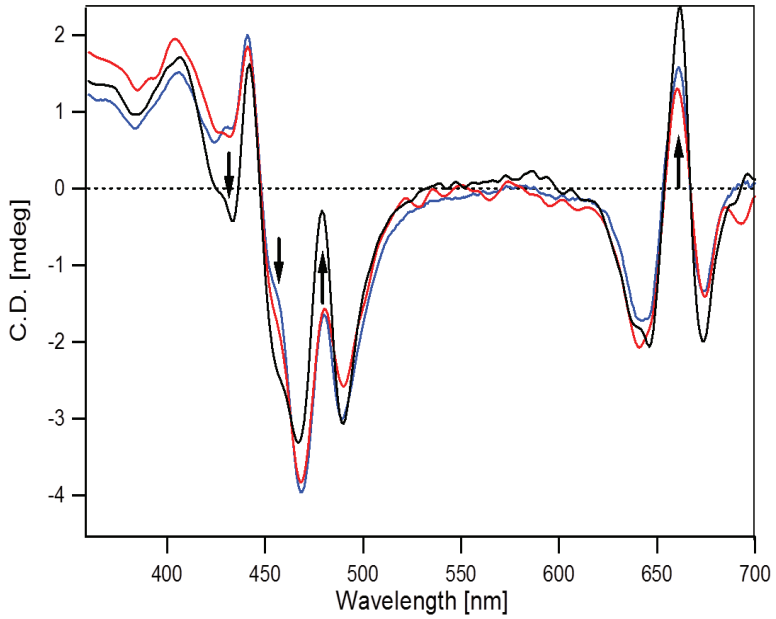

Figure 2.10 CD spectra of LHCII in MGDG: DGDG: SQDG: PG proteoliposomes; PLR of 1:2222, in red, PLR of 1:555, in blue and PLR of 1:65, in black. Arrows indicate the most significant changes for PLR 1:65.

Figure 2.11 presents the CD difference spectrum of proteoliposomes with PLR 1:65 minus PLR 1:555. In the referred CD spectra in Figure 2.10, we can exclude changes due to transitions from a detergent to a lipid environment. We presume that at a PLR of 1:555 the LHCII complexes are involved in weak protein-protein contacts. The CD difference spectrum in Figure 2.11 then shows changes in LHCII conformation and microenvironment that are associated with the transition from a weak to a strong protein-coupling regime. These changes occur at LHCII sites that have been proposed as quencher sites in earlier studies and involve the pigments Chl *a*610, *a*611, *a*612 and Lut1 as will be explained below [4,14,18]. In the CD Q_y region, the bands at (+)662 nm and (-)673 nm are dominated by Chl *a*611-Chl *a*612 interactions [39]. The CD difference spectrum in Figure 11 indicates that those interactions are enhanced at high PLR. The extensive CD study of Akhtar et al. on LHCII in liposomes and detergent micelles concluded that CD changes at (-)437 nm and (+)484 nm are specific to LHCII-LHCII interactions [42]. A negative band at 437 nm, however, is also prominent in the difference spectrum of nanodiscs minus proteoliposomes (Figure 2.8), where the band actually is more pronounced in the nanodisc spectrum. This can be explained by proposing that not only LHCII-LHCII contacts but also LHCII-MSP protein-protein contacts will induce this signature. The 437 nm signature does not correlate with fluorescence quenching since LHCII in nanodiscs retains its fully fluorescent state. The Soret region of the CD difference spectrum in Figure 2.11 further contains additional bands at (-)455, (-)492 and (+)503 nm, of which the latter two signatures have tentatively been attributed to changes in the configuration or micro-environment of lutein 1 (Lut1) [43]. Increased Chl *a*612-Lut1 excitonic interactions could explain the negative contribution to the CD signal at

(-)492 nm [39]. On the other hand, the (-)492 nm band has been attributed to changes in the Neo xanthophyll that protrudes from the LHCII complexes [42] and it is known that the formation of LHCII aggregates is associated with distortion of the Neo polyene chain [14].

Summarizing, the transition from a mild to strong fluorescence-quenched state, reminiscent of the transition from a light-harvesting to a photoprotective state *in vivo*, is associated with CD changes involving enhanced Chl *a*611-*a*612 and Lut1-Chla *a*612 interactions or changes in the Neo environment. These sites correspond with quenching-associated structural changes that have been proposed in various studies [14,17,18,44]. Our results suggest that aggregation-induced LHCII fluorescence quenching at very low protein densities, however, is a different process that does not involve those characteristic CD features and does not reduce the fluorescence more than ~50%. This observation is in agreement with the observation of Holleboom *et al.* that in addition to a Car-Chl coupling-dependent quenching mechanism acting at high protein densities, another Car-Chl independent quenching mechanism is involved in a weak-coupling regime [13]. In the earlier study by Moya *et al.* aggregation-induced LHCII fluorescence quenching was studied in proteoliposomes with much higher protein densities than in our study [32]. They showed aggregation-dependent shortening of the LHCII fluorescence lifetimes from 1.7 to 0.9 ns [32]. We presume that their results reflect the transition from a mild to strong fluorescence-quenched state occurs, and not the transition occurring at the onset of aggregation that we followed in Figure 2.4.

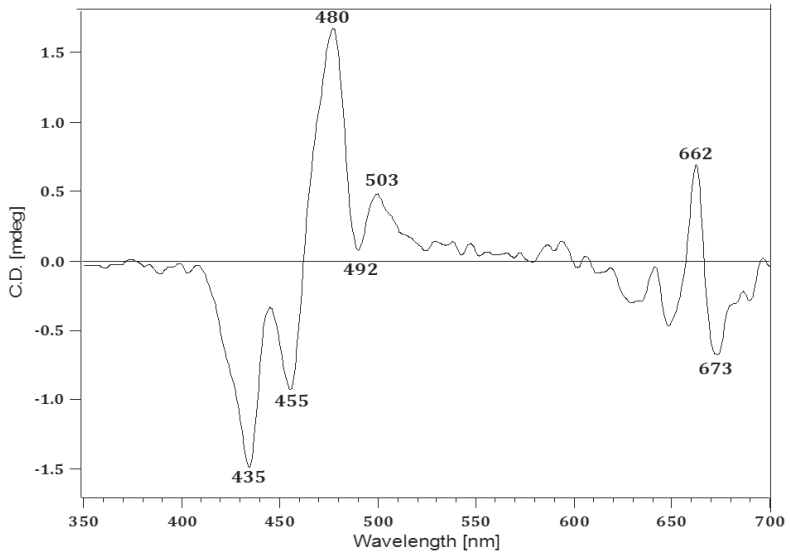

Figure 2.11 CD difference spectrum of LHCII MGDG: DGDG: SQDG: PG proteoliposomes with PLR 1:65–PLR 1:555.

THE ORIENTATION OF LHCII INSERTION IN PREFORMED LIPOSOMES

Finally, we tested if, with our liposome reconstitution method that follows the method of Rigaud, the LHCII complexes would insert in membranes with a preferential orientation [45]. LHCII proteoliposomes with low protein to lipid ratios and LHCII in β-DM as a control were exposed to trypsin or chymotrypsin cleavage. Trypsin is known to cleave part of the N-terminal site of LHCII, while for well-folded LHCII complexes the C-terminal cleavage sites are shielded from cleavage and buried in the hydrophobic membrane phase. Random orientation of LHCII in liposomes should lead to 50% cleavage if half the LHCII have their N-terminal sites oriented inward in the liposome interiors. In contrast, the interactions of trypsin with LHCII in β-DM micelles should lead to 100% cleavage since all LHCII N-terminal sites are accessible. The cleavage experiments were repeated under different trypsin incubation conditions, varying the temperature and incubation times. Figure 2.14 shows a typical SDS-page analysis of a cleavage experiment. Strikingly, for LHCII proteoliposomes only a cleaved product band is observed, suggesting that all proteins are cleaved. For LHCII in β-DM micelles, two cleavage products are found, which indicates that the protein is more exposed in detergent micelles. The two trypsin cleavage products are identified as 25 kDa and 23.5 kDa fragments of N-terminal-cleaved LHCII [46]. The results suggest a strong preferential orientation of LHCII in membranes, with its C-terminal site inserted and its N-terminal site exposed to the liposome exterior. No cleavage products were detected from chymotrypsin, that cleaves the two aromatic-type amino acids tryptophan and phenylalanine, instead of the polar residues lysine and arginine that are cleaved by trypsin as indicated in Figures 2.12 and 2.13.

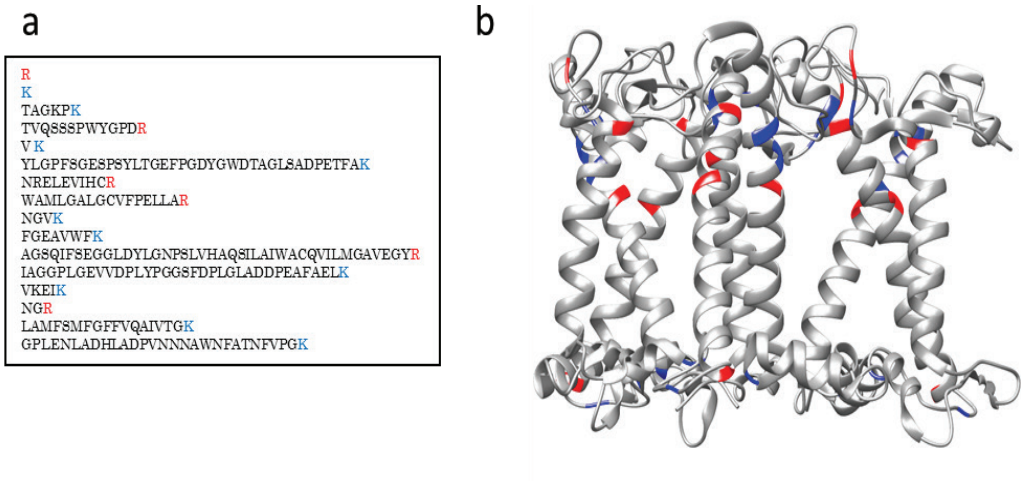

Figure 2.12 Trypsin cleavage sites in LHCII. Arginine (R) in red and lysine (K) in blue.

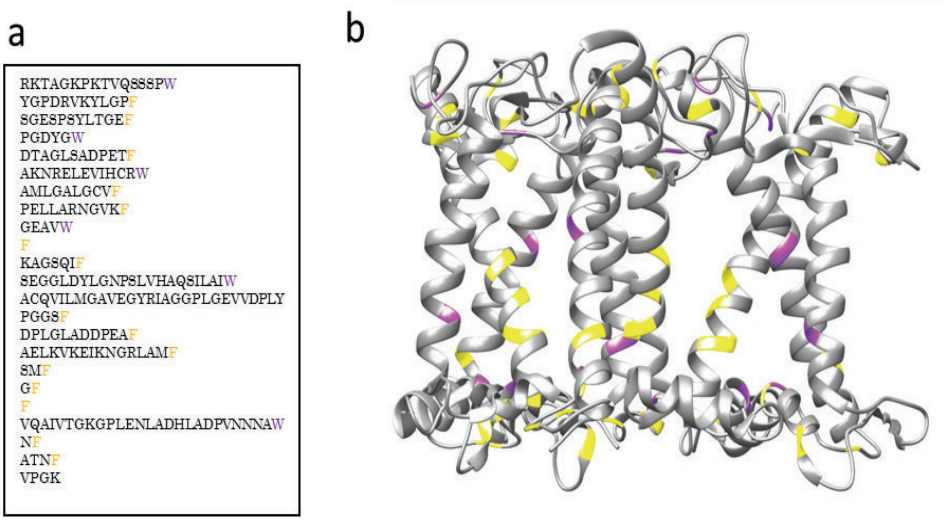

Figure 2.13 Chymotrypsin cleavage sites in LHCII sequence. Tryptophan (W) in purple and phenylalanine (F) in yellow.

Chymotrypsin is unable to cleave the designated sites because the aromatic residues are buried in the hydrophobic phase of the membrane or detergent micelles.

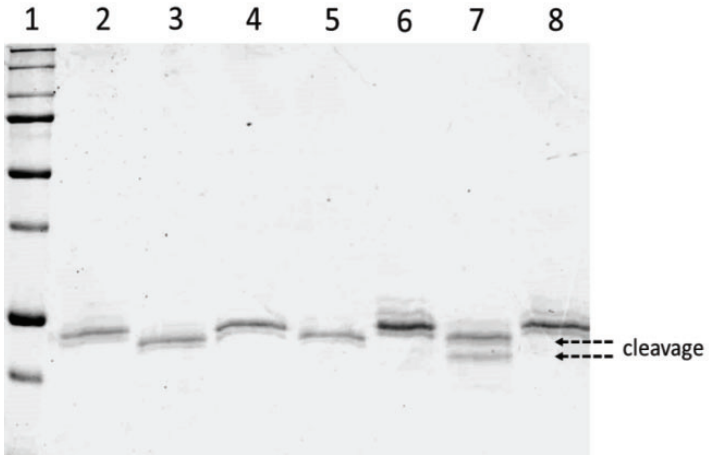

Figure 2.14 SDS-page analysis of enzymatic cleavage experiments. From left to right: 1, marker; 2, LHCII proteoliposomes; 3, LHCII proteoliposomes + trypsin; 4, LHCII proteoliposomes + chymotrypsin; 5, LHCII proteoliposomes with trypsin and chymotrypsin; 6, LHCII in β-DM; 7, LHCII in β-DM + trypsin; 8, LHCII in β-DM + chymotrypsin. Arrows indicate the height of cleavage product bands.

In native thylakoid membranes and in *in vitro* membrane refolding studies, LHCII apoproteins insert in the membrane starting from their C-terminal site that is exposed to the lumen interior [46,47]. To the best of our knowledge, we are the first to observe preferential insertion of folded, native LHCII pigment-protein complexes upon membrane reconstitution. Preferential insertion of membrane proteins from mixed protein-detergent micelles into liposome membranes, as well as membrane insertion of membrane α-helices during folding and assembly *in vivo*, is driven by the hydrophobicity of the protein terminal sites [48,49]. LHCII pigment-protein complexes contain several polar groups at both protein sites, but while at the C-terminal site positively- and negatively-charged residues are in the close distance and may neutralize the net charges, the N-terminal site contains a distinct pattern of positive and negative patches [50]. Such a pattern could

prevent insertion via the N-terminal site. Trypsin cleavage experiments unfortunately only detect interactions at the LHCII N-terminal site. Adding a C-terminal tag by using recombinant LHCII could help to further clarify the direction of LHCII insertion using our reconstitution method.

GENERAL DISCUSSION

The low PLR onset for aggregation-induced LHCII quenching demonstrates that strong attractive forces exist between the LHCII proteins in the membrane. In native membranes, the formation of membrane domains and the presence of MGDG could further promote aggregation by controlling membrane curvature. The low onset for quenching implies that studies using diluted LHCII proteoliposomes should take into account the vesicle dimensions in addition to the PLR because quenched states are already produced when more than one LHCII protein *per vesicle* is present. For larger liposomes, these occasions will occur at lower PLRs. Strong attractive forces in LHCII *in vitro* aggregates are often attributed to head-tail interactions, in which proteins make non-native interfacial protein contacts. Our results however strongly suggest that also under experimental conditions where membrane-embedded LHCII complexes are uniformly oriented attractive protein interactions occur.

We demonstrate that excitation quenching in LHCII membranes is not induced by protein-lipid molecular interactions, but is controlled by the effects of aggregation. At low protein densities, attractive forces between the LHCII complexes cause mild quenching. At very high protein densities, the effect of lateral pressure caused by membrane crowding might produce the conformational changes into more strongly quenched states. While simple LHCII-lipid model systems have many limitations in mimicking native thylakoid membranes, it is interesting to note that they can reproduce the connectivity that is essential for active light-harvesting as well as the strong excitation quenching of photoprotective states [23,32,51]. This notion suggests that lipid physicochemical parameters and the molecular design of LHC complexes are sufficient elements to govern a flexible light-harvesting antenna.

CONCLUSIONS

We demonstrate that LHCII fluorescence quenching is not the result of a specific thylakoid lipid microenvironment, but is driven by LHCII protein-protein interactions. Increasing the PLR of LHCII proteoliposomes decreased the fluorescence and stabilized at a ~50% reduced yield at a PLR of 10^{-3}, indicating (1) that strong LHCII-LHCII attractive interactions occur and (2) that this mild quenching process reaches equilibrium at protein densities of only tens of LHCII trimers per vesicle. The quenching process at the onset of aggregation is distinct from a second transition that occurs at much higher protein densities. A comparison of LHCII proteoliposomes with low and very high protein densities allowed us to detect the excitonic CD changes that are correlated with the second transition from mild to strongly quenched states. The CD changes in the infrared region are attributed to Chl *a*611- *a*612 enhanced interactions, while alterations in the Soret band could originate from Chl-Lut1 or Chl-Neo enhanced interactions. Those sites correlate well with the quencher sites that have been proposed for the LHCII photoprotective switch.

REFERENCES

1. Blankenship RE. Molecular Mechanisms of photosynthesis. (2014).

2. Sunku K, de Groot HJ, Pandit A. Insights into the photoprotective switch of the major light-harvesting complex II (LHCII): a preserved core of arginine-glutamate interlocked helices complemented by adjustable loops. *J Biol Chem*, 288(27), 19796-19804 (2013).

3. Ruban AV, Johnson MP, Duffy CD. The photoprotective molecular switch in the photosystem II antenna. *Biochim Biophys Acta*, 1817(1), 167-181 (2012).

4. Kruger TP, Ilioaia C, Johnson MP *et al.* Controlled disorder in plant light-harvesting complex II explains its photoprotective role. *Biophys J*, 102(11), 2669-2676 (2012).

5. Bode S, Quentmeier CC, Liao PN *et al.* On the regulation of photosynthesis by excitonic interactions between carotenoids and chlorophylls. *Proceedings of the National Academy of Sciences of the United States of America*, 106(30), 12311-12316 (2009).

6. Pandit A, Wawrzyniak P, van Gammeren A, Buda F, Ganapathy S. Nuclear Magnetic Resonance Secondary Shifts of a Light-Harvesting II Complex Reveal Local Backbone Perturbations Induced by Its Higher-Order Interactions. *Biochemistry*, 49(3), 478-486 (2010).

7. Cruz J, Avenson T, Kanazawa A, Takizawa K, Edwards G, Kramer D. Plasticity in light reactions of photosynthesis for energy production and photoprotection. *Journal of experimental botany*, 56(411), 395-406 (2005).

8. Tian L, Dinc E, Croce R. LHCII Populations in Different Quenching States Are Present in the Thylakoid Membranes in a Ratio that Depends on the Light Conditions. *The Journal of Physical Chemistry Letters*, 6(12), 2339-2344 (2015).

9. Petrou K, Belgio E, Ruban AV. pH sensitivity of chlorophyll fluorescence quenching is determined by the detergent/protein ratio and the state of LHCII aggregation. *Biochim Biophys Acta - Bioenergetics*, 1837(9), 1533-1539 (2014).

10. Ilioaia C, Johnson M, Horton P, Ruban A. Induction of Efficient Energy Dissipation in the Isolated Light-harvesting Complex of Photosystem II in the Absence of Protein Aggregation. *Journal of biological chemistry*, 283(43), 29505-29512 (2008).

11. Kirchhoff H. Structural changes of the thylakoid membrane network induced by high light stress in plant chloroplasts. *Philos Trans R Soc Lond B Biol Sci*, 369(1640) (2014).

12. Haferkamp S, Haase W, Pascal AA, van Amerongen H, Kirchhoff H. Efficient Light Harvesting by Photosystem II Requires an Optimized Protein Packing Density in Grana Thylakoids. *The Journal of Biological Chemistry*, 285(22), 17020-17028 (2010).

13. Holleboom C-P, Yoo S, Liao P-N *et al.* Carotenoid–Chlorophyll Coupling and Fluorescence Quenching Correlate with Protein Packing Density in Grana-Thylakoids. *J Phys Chem B*, 117(38), 11022-11030 (2013).

14. Ruban AV, Berera R, Ilioaia C *et al.* Identification of a mechanism of photoprotective energy dissipation in higher plants. *Nature*, 450(7169), 575-578 (2007).

15. Miloslavina Y, Wehner A, Lambrev P *et al.* Far-red fluorescence: A direct spectroscopic marker for LHCII oligomer formation in non-photochemical quenching. *FEBS letters*, 582(25-26), 3625-3631 (2008).

16. Holt NE, Zigmantas D, Valkunas L, Li XP, Niyogi KK, Fleming GR. Carotenoid cation formation and the regulation of photosynthetic light harvesting. *Science*, 307(5708), 433-436 (2005).

17. Pandit A, Reus M, Morosinotto T, Bassi R, Holzwarth A, Holzwarth AR. An NMR comparison of the light-harvesting complex II (LHCII) in active and photoprotective states reveals subtle changes in the chlorophyll a ground-state electronic structures. *Biochim Biophys Acta -Bioenergetics*, 1827(6), 738-744 (2013).

18. Duffy CDP, Pandit A, Ruban A. Modeling the NMR signatures associated with the functional conformational switch in the major light-harvesting antenna of photosystem II in higher plants. *PCCP. Physical chemistry chemical physics*, 16(12), 5571-5580 (2014).

19. Ilioaia C, Johnson MP, Liao P-N *et al.* Photoprotection in Plants Involves a Change in Lutein 1 Binding Domain in the Major Light-harvesting Complex of Photosystem II. *The Journal of Biological Chemistry*, 286(31), 27247-27254 (2011).

20. Chmeliov J, Gelzinis A, Songaila E *et al.* The nature of self-regulation in photosynthetic light-harvesting antenna. *Nature Plants*, 2, 16045 (2016).

21. Chmeliov J, Trinkunas G, van Amerongen H, Valkunas L. Light Harvesting in a Fluctuating Antenna. *Journal of the American Chemical Society*, 136(25), 8963-8972 (2014).

22. Schaller S, Latowski D, Jemioła-Rzemińska M *et al.* Regulation of LHCII aggregation by different thylakoid membrane lipids. *Biochim Biophys Acta - Bioenergetics*, 1807(3), 326-335 (2011).

23. Zhou F, Liu S, Hu Z, Kuang T, Paulsen H, Yang C. Effect of monogalactosyldiacylglycerol on the interaction between photosystem II core complex and its antenna complexes in liposomes of thylakoid lipids. *Photosynthesis Research*, 99(3), 185-193 (2009).

24. Wilk L, Wilk L, Grunwald M, Walla PJ, Walla PJ, Kuhlbrandt W. Direct interaction of the major light-harvesting complex II and PsbS in nonphotochemical quenching. *Proc. Natl. Acad. Sci. USA*, 110(14), 5452-5456 (2013).

25. Pandit A, Pandit N, Shirzad Wasei L *et al.* Assembly of the Major Light-Harvesting Complex II in Lipid Nanodiscs. *Biophysical journal*, 101(10), 2507-2515 (2011).

26. F. Szoka J, AND D. Papahadjopoulus. Procedure for preparation of liposomes with large internal aqueous space and high capture by reverse-phase evaporation. *Proc. Natl. Acad. Sci. USA*, 75(9), 4194-4198, (1978).

27. Graham JM, Harris JR, Rickwood D. In Vitro Techniques Cell Biology Protocols. 201-378 (2006).

28. Butler PJG, Kühlbrandt W. Determination of the aggregate size in detergent solution of the light-harvesting chlorophyll a/b-protein complex from chloroplast membranes. *Proceedings of the National Academy of Sciences*, 85(11), 3797-3801 (1988).

29. Bayburt TH, Sligar SG. Membrane protein assembly into Nanodiscs. *FEBS Letters*, 584(9), 1721-1727 (2010).

30. Webb MS, Green BR. Biochemical and biophysical properties of thylakoid acyl lipids. *Biochim Biophys Acta - Bioenergetics*, 1060(2), 133-158 (1991).

31. Jouhet J. Importance of the hexagonal lipid phase in biological membrane organization. *Frontiers in Plant Science*, 4, 494 (2013).

32. Moya I, Silvestri M, Vallon O, Cinque G, Bassi R. Time-Resolved Fluorescence Analysis of the Photosystem II Antenna Proteins in Detergent Micelles and Liposomes. *Biochemistry*, 40(42), 12552-12561 (2001).

33. Belgio E, Johnson Matthew P, Jurić S, Ruban Alexander V. Higher Plant Photosystem II Light-Harvesting Antenna, Not the Reaction Center, Determines the Excited-State Lifetime-Both the Maximum and the Nonphotochemically Quenched. *Biophysical Journal*, 102(12), 2761-2771 (2012).

34. Mansoor SE, Palczewski K, Farrens DL. Rhodopsin self-associates in asolectin liposomes. *Proc. Natl. Acad. Sci. USA*, 103(9), 3060-3065 (2006).

35. Lambrev PH, Schmitt F-J, Kussin S *et al.* Functional domain size in aggregates of light-harvesting complex II and thylakoid membranes. *Biochim Biophys Acta - Bioenergetics*, 1807(9), 1022-1031 (2011).

36. Lambrev PH, Varkonyi Z, Krumova S *et al.* Importance of trimer-trimer interactions for the native state of the plant light-harvesting complex II. *Biochim. et Biophys. Acta*, 1767(6), 847-853 (2007).

37. Hobe S. Pytulla S, Kuhlbrandt W and Paulsen H. Trimerization and crystallization of reconstituted light-harvesting chlorophyll a/b complex. *The EMBO Journal*, 13(15), 3423-3429 (1994).

38. Yang C, Boggasch S, Haase W, Paulsen H. Thermal stability of trimeric light-harvesting chlorophyll a/b complex (LHCIIb) in liposomes of thylakoid lipids. *Biochim. et Biophys. Acta*, 1757(12), 1642-1648 (2006).

39. Georgakopoulou S, van der Zwan G, Bassi R, van Grondelle R, van Amerongen H, Croce R. Understanding the Changes in the Circular Dichroism of Light Harvesting Complex II upon Varying Its Pigment Composition and Organization. *Biochemistry*, 46(16), 4745-4754 (2007).

40. Yang C, Boggasch S, Haase W, Paulsen H. Thermal stability of trimeric light-harvesting chlorophyll a/b complex (LHCIIb) in liposomes of thylakoid lipids. *Biochim. et Biophys. Acta - Bioenergetics*, 1757(12), 1642-1648 (2006).

41. Liu Z, Yan H, Wang K *et al.* Crystal structure of spinach major light-harvesting complex at 2.72 Å resolution. *Nature*, 428(6980), 287-292 (2004).

42. Akhtar P, Pawlak K, Kovacs L *et al.* Pigment Interactions in Light-harvesting Complex II in Different Molecular Environments. *Journal of biological chemistry*, 290(8), 4877-4886 (2015).

43. Ilioaia C, Johnson MP, Horton P, Ruban AV. Induction of Efficient Energy Dissipation in the Isolated Light-harvesting Complex of Photosystem II in the Absence of Protein Aggregation. *The Journal of Biological Chemistry*, 283(43), 29505-29512 (2008).

44. Chmeliov J, Bricker W, Lo C, Jouin E, Valkunas L, Ruban A. An 'all pigment' model of excitation quenching in LHCII. *PCCP. Physical chemistry chemical physics*, 17(24), 15857-15867 (2015).

45. Rigaud J-L, Lévy D. Reconstitution of Membrane Proteins into Liposomes. In: *Methods in Enzymology*. (Academic Press, 2003) 65-86.

46. Zapf T, Tan C-W, Reinelt T *et al.* Synthesis and Functional Reconstitution of Light-Harvesting Complex II into Polymeric Membrane Architectures. *Angewandte Chemie (International ed.)*, 54(49), 14664-14668 (2015).

47. Kuttkat A, Grimm R, Paulsen H. Light-harvesting chlorophyll a/b-binding protein inserted into isolated thylakoids binds pigments and is assembled into trimeric light- harvesting complex. *Plant Physiology*, 109(4), 1267-1276 (1995).

48. Rigaud J-L, Pitard B, Levy D. Reconstitution of membrane proteins into liposomes: application to energy-transducing membrane proteins. *Biochimica et Biophysica acta. Bioenergetics*, 1231(3), 223-246 (1995).

49. Engelman DM, Steitz TA. The spontaneous insertion of proteins into and across membranes: The helical hairpin hypothesis. *Cell*, 23(2), 411-422 (1981).

50. Standfuss R, van Scheltinga ACT, Kuhlbrandt W, Standfuss J, Lamborghini M, Kühlbrandt W. Mechanisms of photoprotection and nonphotochemical quenching in pea light-harvesting complex at 2.5 Å resolution. *EMBO Journal*, 24(5), 919-928 (2005).

51. Sun R, Liu K, Dong L, Wu Y, Paulsen H, Yang C. Direct energy transfer from the major antenna to the photosystem II core complexes in the absence of minor antennae in liposomes. *Biochim Biophys Acta - Bioenergetics*, 1847(2), 248-261 (2015).